Untethered Hovering Flapping Flight of a 3D-Printed Mechanical Insect

Charles Richter**
Cornell University

Hod Lipson*,**
Cornell University

Keywords
3D printing, ornithopter, micro air vehicle, untethered hovering, insect flight

A version of this paper with color figures is available online at http://dx.doi.org/10.1162/artl_a_00020. Subscription required.

Abstract This project focuses on developing a flapping-wing hovering insect using 3D-printed wings and mechanical parts. The use of 3D printing technology has greatly expanded the possibilities for wing design, allowing wing shapes to replicate those of real insects or virtually any other shape. It has also reduced the time of a wing design cycle to a matter of minutes. An ornithopter with a mass of 3.89 g has been constructed using the 3D printing technique and has demonstrated an 85-s passively stable untethered hovering flight. This flight exhibits the functional utility of printed materials for flapping-wing experimentation and ornithopter construction and for understanding the mechanical principles underlying insect flight and control.

1 Introduction

Hovering flapping flight of insects and birds has long fascinated scientists and engineers, but only in the last decade has it been successfully demonstrated by man-made flying machines. Unlike forward flight, hovering flapping flight poses several special challenges. First, there has yet to emerge an established body of theoretical and experimental work on the unsteady aerodynamics of flapping wing flight for the purposes of wing design. Second, hovering flapping flight of insects and birds is generally unstable and requires a sophisticated solution to maintain an upright flying position [15, 16]. Third, the energy density of batteries was insufficient for the power demands of hovering flight until small lithium-based batteries became widely available. However, with the improvement of electrical power solutions, a number of successful hovering ornithopters have been developed with a variety of wing designs. This project utilizes existing solutions to the power and stability problems and uses 3D printing as a novel approach to designing and manufacturing the key aerodynamic component: the wings.

Thus far, producing effective flapping wings for research and ornithopter construction has been a time-consuming and delicate process taking days or longer to complete. The 3D printing technique allows wings to be produced in a matter of minutes, dramatically reducing the time of each design cycle. Overcoming this barrier to experimentation will allow a comprehensive study of lift production for a wide variety of wing shapes, including those replicating real insect wings.

* Contact author.
** Computational Synthesis Laboratory, 239 Upson Hall, Sibley School of Mechanical & Aerospace Engineering, Cornell University, Ithaca, NY 14853. E-mail: car45@cornell.edu (C.R.); hod.lipson@cornell.edu (H.L.)

A comprehensive understanding of flapping-wing aerodynamics and hovering flight will become increasingly important as ornithopters shrink to the scale of real insects, where some advantages of flapping-wing flight are realized [7]. These advantages include efficiency and maneuverability improvements over fixed and rotary wing aircraft at low Reynolds numbers as well as the suitability of microscale actuators to producing vibrating motion for flapping rather than rotary motion for traditional propellers [12, 20]. Maneuverable, low-power micro air vehicles have a wide range of applications, including mapping, surveillance, and search-and-rescue operations, where these properties of small size and ability to maneuver in tight spaces are vital, and those in thin extraterrestrial atmospheres, where low Reynolds numbers occur [11]. Micro air vehicles also present a challenging synthesis of many areas of engineering, including materials, actuators, electronics, control, vision, and guidance [8, 9]. This project has demonstrated the viability of 3D-printed aerodynamic components for experimentation and for use in a real ornithopter on the size scale of the smallest current designs (Figure 1).

1.1 Review of Existing Work

The existing work that has influenced this project includes a variety of successful ornithopter designs and some research on the dynamics and control of insect flight (Table 1). This project is a continuation of an earlier ornithopter design project by Floris van Breugel of the Cornell Computational Synthesis Laboratory. Van Breugel's design used four motors to drive eight wings and featured passively stable flight dynamics using a set of damping sails above and below the body of the aircraft. This model had a mass of 24 g and demonstrated stable hovering flight of over 30 s in 2007. Broad goals for the current project were to achieve a comparable flight time using this system of passive stability in a vehicle under 10 g.

Several other successful designs currently exist, including the series of DelFly ornithopters, which are radio controlled using tail configurations resembling fixed-wing aircraft, and the AeroVironment Nano Air Vehicle, which achieves control using active wing control. The Harvard Microrobotics Laboratory has also produced ornithopters weighing 60 mg using piezoelectric actuators and insectlike passive wing pitching, but requiring a tether for power and stability.

There have also been recent developments in the understanding of insect flight [2, 6, 13, 18]. These studies have explored one mechanism of passive wing deflection in insect flight that is essential to the simplicity of some ornithopter designs. They have shown that some insect wings deflect to an angle of incidence of 45°, which is thought to be optimal for lift production of a flat-plate wing. These findings have also given rise to hypotheses explaining forward thrust, flight maneuvers,

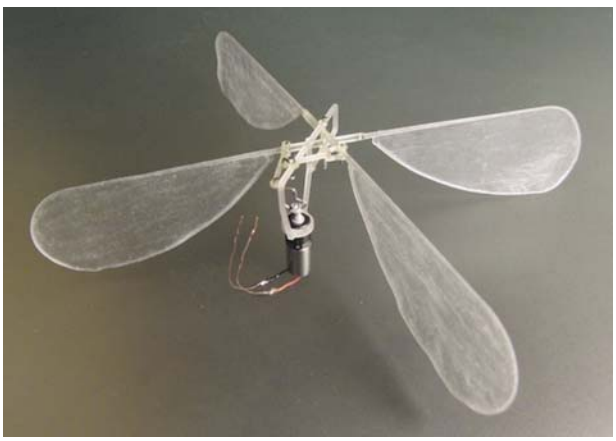

Figure 1. 3D-printed elements of flapping-hovering insect.

Table 1. Characteristics of existing ornithopter designs.

Design	Year	Mass (g)	Span (cm)	Wings	Hover time (s)	Features
Mentor [21]	2002	580	36	4	>60	Nitromethane fuel
DelFly II [5]	2006	16.07	28	4	480	Camera, R/C
van Breugel [17]	2007	24.2	45	8	33	Passively stable
Chronister [3]	2007	3.3	15	4	Unknown	R/C
Wood [19]	2007	0.060	3	2	N/A	Piezoelectric power
DelFly Micro [5]	2008	3.07	10	4	N/A	Camera, R/C
NAV [1]	2009	10 (est.)	7.5 (est.)	2	20	Active wing pitching
Richter (this work)	2010	3.89	14.3	4	85	3D printed parts, wings

and disturbance rejection, and experiments have been designed to examine these hypotheses using the ornithopter as a test bed.

One primary goal of this project was to produce a hovering ornithopter with as many 3D-printed components as possible. An Objet EDEN260V printer and the Objet FullCure 720 material were used to produce all printed components. This material costs roughly 0.22 USD per gram, and the EDEN 260V prints with a resolution of 42 μm on the x and y axes and 16 μm on the z axis. At first, only the fuselage, hinges, and pushrods were printed; however, a method of printing entire one-piece wings was soon developed.

First attempts at wing construction were aimed at recreating the wings of the van Breugel design, using a carbon fiber rod as the main strut, polyethylene terephthalate (PET) stiffening ribs, and a Mylar film wing surface. Two examples of this early printed type can be seen in the upper left corner of Figure 2. The carbon fiber rod was to extend out of a 3D-printed hinge, but after several design iterations, the hinge, strut, and stiffening ribs were combined into a single printed piece. When further experimentation revealed that a durable thin film could be printed using only two

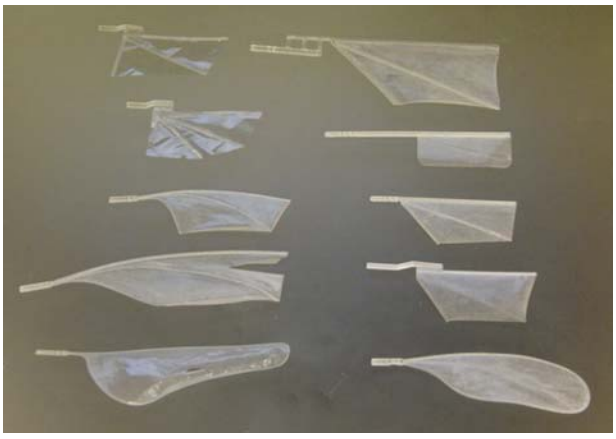

Figure 2. A variety of wing shapes for experimentation.

layers of printed material, this film was used instead of Mylar as the wing surface, and the first one-piece printed wings were made. Figure 2 shows many conventional and biologically inspired printed wings.

1.2 Printed-Wing Construction

The printed wings of the ornithopter are composed of three functional elements: the central beam, the surrounding frame, and the thin film wing surface. Figure 3 shows the parts of the dual wing used in the full ornithopter design. The central beam is the most rigid portion of the wing and contains the pivot point as well as the attachment holes for the connecting rods. Whereas some designs require a bushing or dedicated hinge, 3D printing allows the hinge to be incorporated into the main beam design. Furthermore, the FullCure 720 material features relatively low friction against the stainless steel 0.5-mm piano wire hinge pins when lubricated with a drop of medium-viscosity oil. The holes for the pivot points were designed with a 0.6-mm diameter to provide an adequate gap for low-friction operation. This technique eliminates the need for a heavy bushing or complex assembly.

The outer frames of the wings are attached to the ends of the beam. The outer frames determine the flexibility of the wings and the deflection properties during flapping. The outer frames were defined in the CAD model as lofted curves connecting circular cross sections. By varying the radius of the circular cross sections at various points along the frame, the overall stiffness and flexibility patterns of the wing could be tuned.

The thin wing surface is a flexible film that extends through the area inside the outer frame. The surface has a thickness of 40 μm, which is achieved by depositing two layers of material. The ability of the printer to print such a thin flexible film is the development that made a one-piece printed wing possible. While it is possible to print a thinner film using a single layer, wings constructed with a single-layer surface are extremely delicate and tend to tear upon vigorous flapping. Chamfers were used to counter the tendency of the wing film to tear at points of discontinuous geometry, such as the edge where the film joins the frame.

One practical element of 3D printing technology is the use of a gelatinous material to support the structure during printing. Therefore, removing the support material is an important step in the manufacturing process, especially with delicate features such as the thin wing's surface. Common methods used to remove support material include dissolving it in sodium hydroxide and spraying it off with pressurized water. However, both of these methods have limitations due to the delicacy of the thin film. When a printed wing is soaked in liquid for any period of time, it tends to curl up or warp. That can be partially corrected by pressing it flat and allowing it to dry. However, the moisture tends to leave some permanent warping of the wing shape. The method of spraying pressurized water is also difficult because extreme care must be taken to avoid tearing the wing film. Again, the moisture tends to warp the wing shape. The best method thus far has been to place the wing on a clean surface with some elasticity, such as a dense rubber mat, and scrape the support material away using

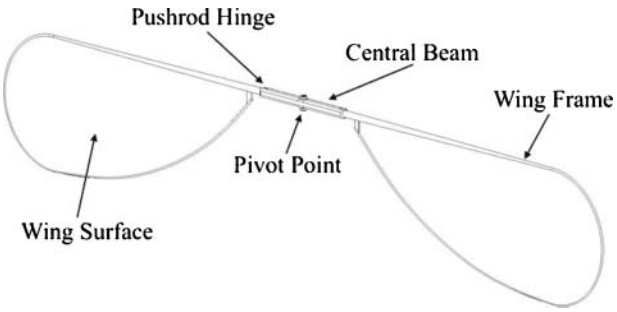

Figure 3. Parts of the one-piece printed wing.

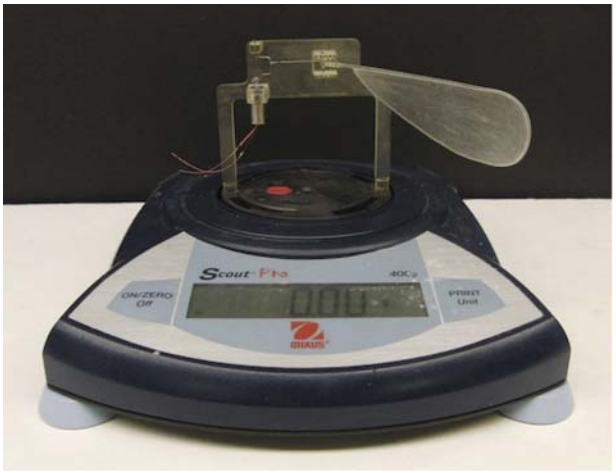

Figure 4. Experimental test setup on the lab scale.

a dull blade. Any residual material can be removed by wiping with a cloth moistened with water or rubbing alcohol. This is the fastest and most successful method for removing support material from the thin wing film.

1.3 Wing Design

At the beginning of the project, the wing design process focused on narrowing the vast design space to a size scale that was appropriate for the motors available and desired weight of the vehicle. During initial testing, key wing design features were identified that helped produce the ideal shapes and deflections when flapping. Testing of a wide variety of wing shapes, sizes, and structures was carried out by powering them with a small DC gear motor using a DC power source. The lift of each wing was measured using a custom attachment for a digital lab scale, and flapping behavior was analyzed using a high-speed camera capturing 1000 frames per second. Figures 4 and 5 show the experimental apparatus.

The wing size partially determines several important variables, including the mass and surface area, which in turn determine how fast the wings can flap for a given power input. For the motor chosen for this project (a GM15 gear motor available from Solarbotics.com with 25:1 gear reduction) and the power expected from a pair of lithium-polymer batteries (7.4 V, 200 mA), the best-performing single wing of all wing designs tested had a length of 80 mm and a maximum chord of 30 mm. The overall weight of the wing was approximately 0.3 g, and the thickness of the wing film

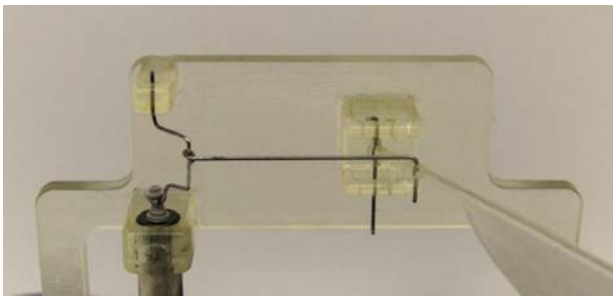

Figure 5. Close-up of test setup mechanism.

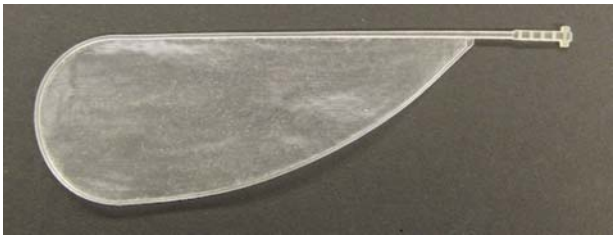

Figure 6. The most successful wing design during testing.

was 40 μm. This wing flapped at approximately 30 Hz through an angle of 110° and produced a maximum lift of 2.92 g. This wing design is shown in Figure 6.

The wing structure is important to proper deflection and wing shape during flapping. For maximum lift, the wing should deflect to an angle of attack of roughly 45° at the middle of the stroke. This angle of attack can be tuned by adjusting the flexibility of the main wing strut and the ribs that stiffen the interior of the wing. Thus far, successful wing designs have been created with and without wing ribs.

One major problem associated with simple deflecting wings is that they do not deflect as flat plates. Instead, the leading edge tends to remain vertical rather than flexing torsionally, while the wing surface bends away underneath it. This behavior creates an inverted camber shape that is undesirable. Several methods were explored to overcome this problem. The most effective solution was to extend the wing frame all the way around the tip of the wing. This design forced the leading edge to twist when the wing deflected, thus maintaining a roughly continuous slope across the chord of the wing near the tip. In other words, the tip of the wing behaved more like a flat plate, with the entire wing deflecting to the proper angle rather than just the lower half.

Wing ribs have also been used to control the deflection patterns and add stiffness in certain directions. Various rib designs were tested featuring rectilinear patterns as well as curved patterns inspired by the wings of dragonflies and other insects. However, the current design does not feature stiffening ribs. Figure 7 shows a top-down view of a wing deflecting during flapping tests on the experimental setup. This general wing design, while not optimal, was deemed satisfactory for use in the challenge of building a full ornithopter using 3D-printed wings. A new double-ended version of this wing shape was produced for use in the full ornithopter.

1.4 Full Ornithopter Design

Once a satisfactory wing design was obtained, it was implemented in the four-wing vehicle. The wing chosen for this purpose was the ribless design that produced the greatest lift. A fuselage was designed to hold the motor, crank, and wing hinge. Care was taken to place the motor as close as possible to the wing pivot point to center the mass.

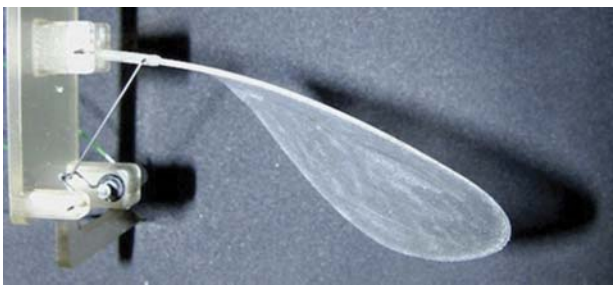

Figure 7. Flash photo showing deflection while flapping.

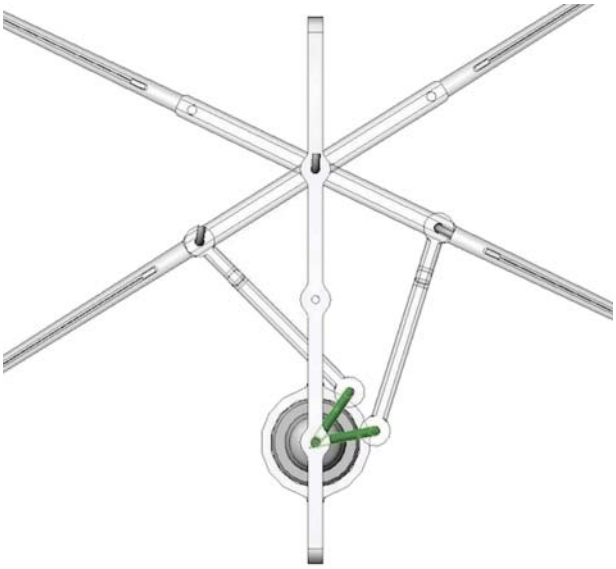

Figure 8. Top view of ornithopter mechanism showing offset-crank geometry.

The wings are driven by a crankshaft connected to the motor's gearbox. In order to drive the wings in a roughly symmetrical motion, the crankshaft includes two attachment points for the connecting rods powering the left and right wings. These two attachment points are roughly 30° out of phase from each other to compensate for the asymmetry of the crank position at any given point in the stroke. Figures 8 and 9 show this offset-crank mechanism, which is similar to the DelFly I design [4] and many toy ornithopters.

The ornithopter was tested first using a DC power source and a fishing line tether to verify proper operation of the crank mechanism and proper flapping behavior of the wings. The crank is designed to flap each of the four wings through roughly 80°, and when the flexibility of the wings is included, this angle is enough to allow the wings to *clap and fling* at the end of each stroke. The

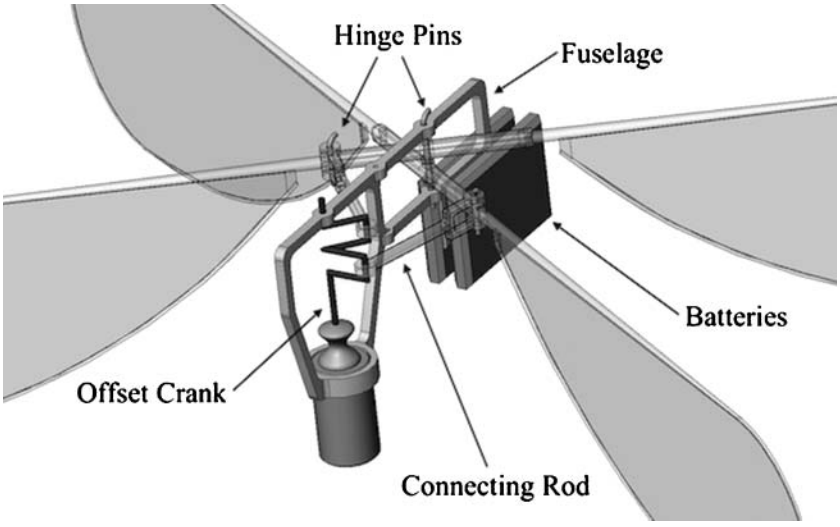

Figure 9. Large view of ornithopter mechanism.

clap-and-fling phenomenon may aid in lift production [10]. Figure 10 shows a photo of a tethered flight test showing ideal wing deflection of roughly 45°. In this test configuration, the ornithopter was able to lift up to 1.5 g of payload, which is roughly equivalent to the mass of batteries required for flight.

Once the ornithopter was able to support a payload while flying on the tether, it was outfitted with batteries, and untethered flight tests began. Two 10-mA h lithium-polymer batteries were used to power the motor and were attached on the opposite side of the motor to balance the mass. The other feature required for untethered flight is a set of thin foam damping sails attached to a thin carbon fiber rod above and below the fuselage to maintain an upright flying position. This method of achieving passive stability was developed by van Breugel and is replicated here [17].

1.5 Passive Stability

The stabilizing sails shown in Figure 11 are designed to maintain stability and keep the ornithopter in an upright orientation. Without sails, the ornithopter tends to tip over, causing a horizontal acceleration and loss of upward lift. However, when the sails are attached, the larger top sail provides a righting force to counter the tendency to tip over, while the bottom sail dampens any pendulum-like oscillations. If launched upside down, the ornithopter will right itself, demonstrating the robustness of the design.

1.6 Lift and Power Characterization

The four-wing configuration was evaluated in a series of experiments to characterize lift and power performance. A test apparatus was designed to replicate the exact geometry and kinematics of the ornithopter fuselage; however, a more powerful motor was selected in order to flap the wings at a steady frequency for extended periods without overheating. For this purpose, the Mabuchi FF-050 motor and BaneBots 11:1 gearbox were used. The four-wing test setup was mounted to a laboratory scale to measure the average lift force and is shown in Figure 12.

Five identical sets of wings were 3D-printed, and each set was tested individually. During each test, the wings were flapped at a range of speeds while voltage, current, frequency, and mean lift force were recorded. Frequency was measured using a stroboscope, while voltage and current were measured using multimeters. The power required to drive the motor and linkage mechanism alone (without wings) was also recorded over a range of frequencies. At each frequency, this value was subtracted from the total power supplied to the system to give a meaningful measurement of the inertial and aerodynamic power demands of flapping lift production.

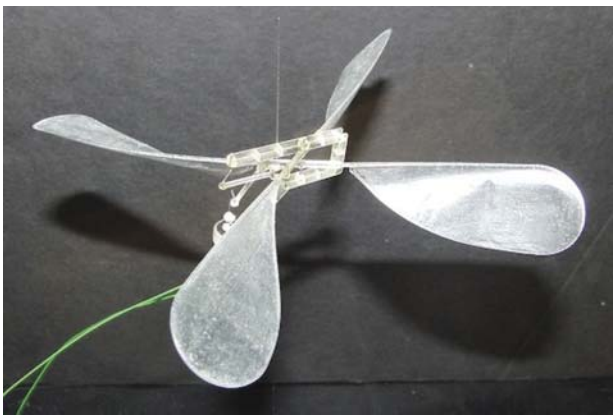

Figure 10. Wing deflection in a tethered flight test.

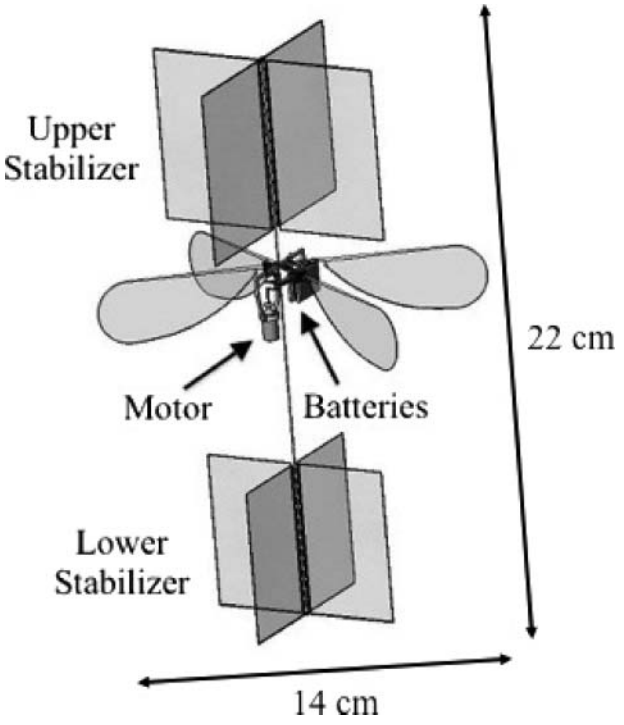

Figure 11. Final configuration of complete ornithopter.

The plots in Figures 13 and 14 show the lift force as a function of frequency and flapping power. The dashed line represents the mass of the complete ornithopter, broken down in Figure 15, which is the lift required for hovering. The standard deviations in these experiments, represented by the error bars in Figures 13 and 14, are very small. The mean standard deviation of lift force across all frequencies of flapping in these experiments was just 1.53%, indicating excellent consistency among

Figure 12. Four-wing test stand precisely replicating the geometry and kinematics of the real ornithopter fuselage for the purpose of characterizing lift and power performance of the four-wing configuration.

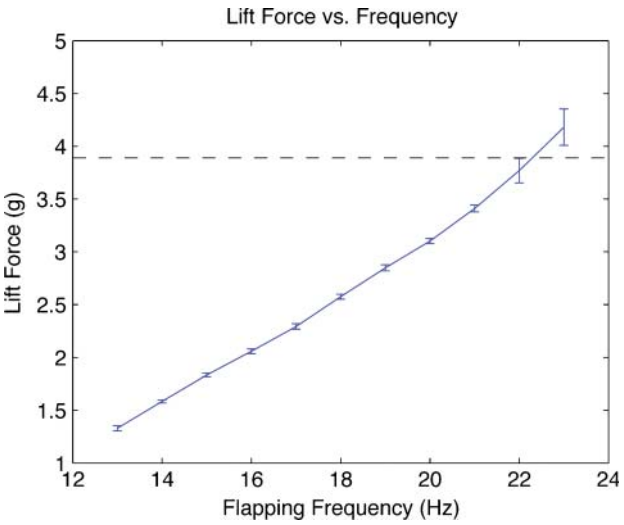

Figure 13. Average lift produced by the four-winged ornithopter configuration as a function of flapping frequency in five independent trials with error bars showing standard deviation.

3D-printed copies of the same wing design. This consistency also reflects the precision available for tuning the wing structure, which makes 3D printing a versatile and powerful technique for wing experimentation.

2 Conclusions

This project has yielded several significant results thus far. First, wing tests and the hovering demonstration have validated the concept of a printed ornithopter. This method of construction has greatly accelerated the design cycle, since a set of wings can be printed in less than 30 min, and a complete set of ornithopter parts can be printed in 60 min. Thus, several design iterations can be tested per day.

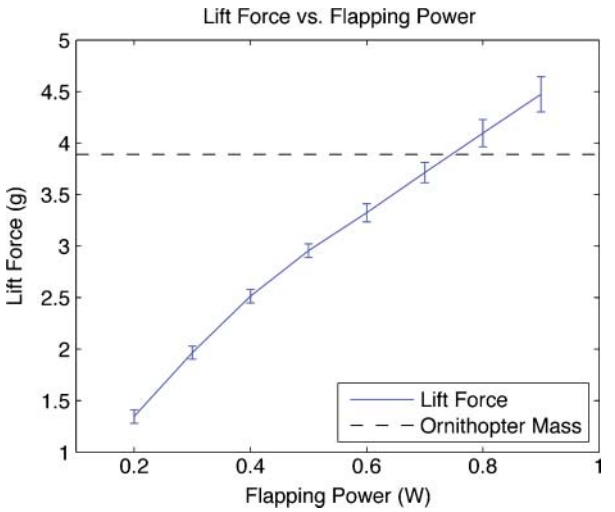

Figure 14. Average lift as a function of flapping power, defined as the total power applied to the motor minus the power required to drive the motor and linkage mechanism alone at the same frequency, in five independent trials, with error bars indicating standard deviation.

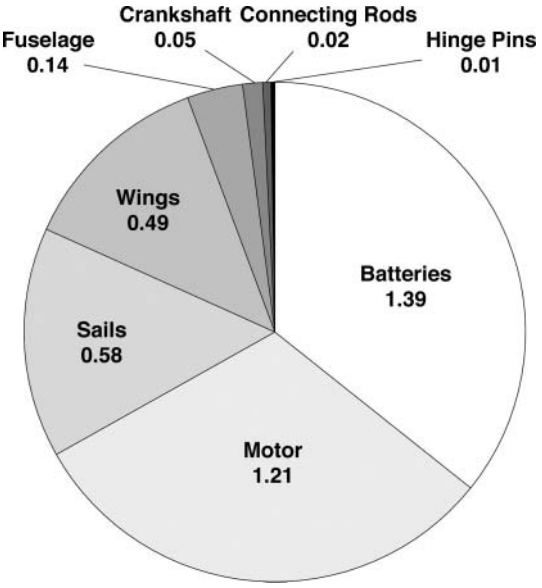

Figure 15. Breakdown of total mass (3.89 g).

The Objet FullCure 720 material has some limitations, particularly in its mechanical properties. It is not as light or as stiff as carbon fiber or balsa wood, which are the main alternative options for wing struts. Therefore, printed wings do not store as much energy when they flex, and energy is lost to friction during each wing stroke. Different strut cross sections will be tested to improve the stiffness per unit volume of material.

Other limitations of the 3D printed material include a tendency of thin wings to curl up after a period of days, rendering them useless. This problem can be corrected by storing wings between flat plates or in the pages of a book, though that requires disassembly. Thin wings also tend to develop small tears after minutes of vigorous flapping. However, this problem can be partially prevented with chamfered edges along the wing frame to avoid discontinuous geometry.

Experimentation with wing designs has begun to uncover some of the features and parameters of successful wings for this size and power scale. The GM15 motor seems to be well matched to wings that are approximately 80–100 mm long from base to tip with a chord length of 30–40 mm when it is running at a power of 1.5 W (typical power consumption during flight). If the wing strut is extended further, then the drag of the wing acts along a longer lever arm, slowing down the rate of flapping and reducing lift.

One very successful design feature is the wing frame that extends around the wingtip. This feature helps maintain a continuous wing slope at the tip of the wing and helps approximate the flat-plate airfoil cross section of many hovering insects. The continuous wingtip frame was a design borrowed from the structure of dragonfly wings, which exhibit ideal shape and deflection at the wingtips. Overall, the use of 3D printing to create flexible wings that are aerodynamically functional is the main accomplishment of this project and will be one area for future improvement. The complete 3D-printed ornithopter is shown in Figures 16 and 17 and is shown hovering in Figure 18.

3 Future Work

A long-term project utilizing a hovering ornithopter will be to test hypotheses of insect propulsion and control. This project will be carried out by building wings with a nominal bias of several degrees

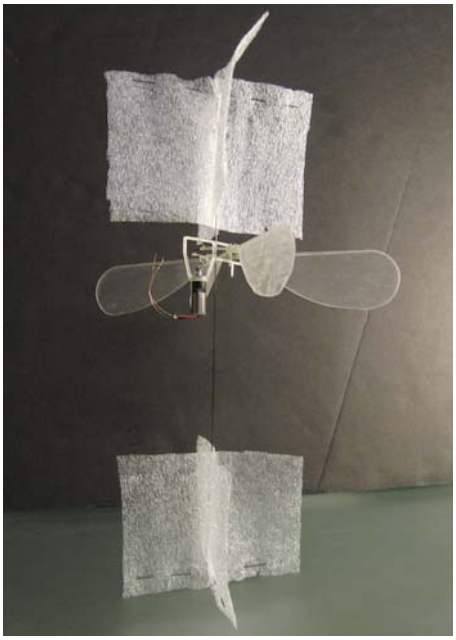

Figure 16. Final design with sails for passive stability.

built into the angle of incidence to produce forward thrust or turning maneuvers. If successful, these principles could form the basis of hovering ornithopter control.

Another project planned for the future is to perform a detailed study using 3D-printed wings to develop analytical models predicting wing performance. The lift of many different wing designs will be measured to identify relationships between the major variables involved in lift production, such as wing length, chord, surface area, flapping frequency, and parameterized shape. This data will then be mined for analytical relationships using the Eureqa software [14]. These laws will then be compared with current designs to evaluate the model and ultimately produce the best possible wings.

Finally, another ornithopter will be designed using 3D-printed wings and other parts that is still smaller and lighter and is composed of an even greater proportion of printed components.

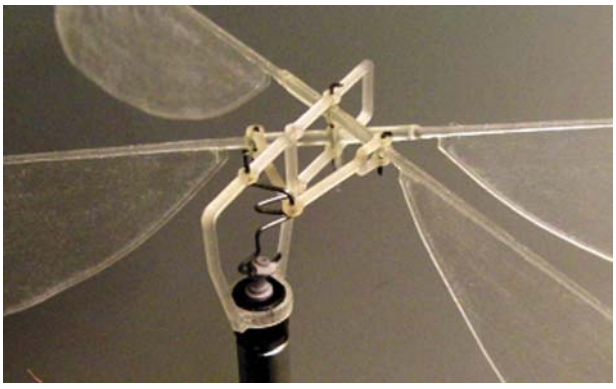

Figure 17. Ornithopter mechanism close-up.

(a)

(b)

(c)

Figure 18. Ornithopter taking flight and hovering in time-series images (a), (b), and (c).

Acknowledgments

This work was supported in part by the U.S. National Science Foundation (NSF) Grant ECCS 0941561 on Cyber-enabled Discovery and Innovation (CDI). We thank Leif Ristroph, Itai Cohen, and Jane Wang for useful discussions.

References

1. AeroVironment (2009). *DARPA awards AeroVironment Phase II contract extension for nano air vehicle development program*. Available at http://www.avinc.com/downloads/NAVPRLongDARPAV4.doc.pdf (accessed April 2010).
2. Bergou, A. J., Xu, S., & Wang, Z. J. (2007). Passive wing pitch reversal in insect flight. *Journal of Fluid Mechanics*, *591*, 321–337.
3. Chronister, N. (2010). *Micro air vehicle ornithopters*. Available at http://www.ornithopter.org/history.mav.shtml (accessed April 2010).
4. de Croon, G. C. H. E., de Clerg, K. M. E., Ruijsink, R., Remes, B., & de Wagter, C. (2009). Design, aerodynamics, and vision-based control of the DelFly. *International Journal of Micro Air Vehicles*, *1*(2), 71–97.
5. DelFly. (2010). Available at http://www.delfly.nl/ (accessed April 2010).
6. Dickinson, M. H., Lehmann, F., & Sanjay, P. (1999). Wing rotation and the aerodynamic basis of insect flight. *Science*, *284*, 1954–1960.
7. Ellington, C. P. (1999). The novel aerodynamics of insect flight: Applications to micro-air vehicles. *Journal of Experimental Biology*, *202*(23), 3439–3448.
8. Floreano, D., Zufferey, J. C., Srinivasan, M., & Ellington, C. (Eds.). (2010). *Flying insects and robots*. Berlin: Springer.
9. Karpelson, M., Wei, G. Y., & Wood, R. J. (2008). A review of actuation and power electronics options for flapping-wing robotic insects. In *IEEE International Conference on Robotics and Automation*.
10. Lehmann, F., Sane, S. P., & Dickinson, M. (2005). The aerodynamic effects of wing-wing interaction in flapping insect wings. *Journal of Experimental Biology*, *208*, 3075–3092.
11. Michelson, R., & Naqvi, M. (2003). Extraterrestrial flight (entomopter-based Mars surveyor). In *von Karman Institute for Fluid Dynamics RTO/AVT lecture series on low Reynolds number aerodynamics on aircraft including applications in emerging UAV technology*. Brussels, Belgium.
12. Pesavento, U., & Wang, Z. J. (2009). Flapping wing flight can save aerodynamic power compared to steady flight. *Physical Review Letters*, *103*(11), 118102.
13. Ristoph, L., Berman, G. J., Bergou, A. J., Wang, Z. J., & Cohen, I. (2009). Automated hull reconstruction motion tracking (HRMT) applied to sideways maneuvers of free-flying insects. *Journal of Experimental Biology*, *212*, 1324–1335.
14. Schmidt, M., & Lipson, H. (2009). Distilling free-form natural laws from experimental data. *Science*, *324*(5923), 81–85.
15. Sun, M., & Xiong, Y. (2005). Dynamic flight stability of a hovering bumblebee. *Journal of Experimental Biology*, *208*, 447–459.
16. Taylor, G. K., & Thomas, A. L. R. (2003). Dynamic flight stability in the desert locust *Schistocerca gregaria*. *Journal of Experimental Biology*, *206*, 2803–2829.
17. van Breugel, F., Regan, W., & Lipson, H. (2008). From insects to machines: A passively stable, untethered flapping-hovering micro air vehicle. *IEEE Robotics and Automation Magazine*, *15*, 68–74.
18. Wang, Z. J. (2005). Dissecting insect flight. *Annual Review of Fluid Mechanics*, *37*, 183–210.
19. Wood, R. J. (2008). The first takeoff of a biologically-inspired at-scale robotic insect. *IEEE Transactions on Robotics*, *24*, 341–347.
20. Woods, M. I., Henderson, J. F., & Lock, G. D. (2001). Energy requirements for the flight of micro air vehicles. *Aeronautical Journal*, *105*(1045), 135–149.
21. Zdunich, P., Bilyk, D., Mac Master, M., & Loewen, D. (2007). Development and testing of the Mentor flapping-wing micro air vehicle. *Journal of Aircraft*, *44*, 1701–1711.